Validation of a Net Active Debris Removal simulator within parabolic flight experiment

Cercós, L*, Stefanescu, R.*, Medina, A.*,
Benvenuto, R.**, Lavagna, M.**, González, I. ***, Rodríguez, N.***, Wormnes, K.****

* GMV, Spain
e-mail: lcercos@gmv.com, rmstefanescu@gmv.com, amedina@gmv.com

** University Polytechnic of Milano, Italy
e-mail: riccardo.benvenuto@polimi.it, michelle.lavagna@polimi.it

*** PRODINTEC Technology Centre, Spain
e-mail: ige@prodintec.com, nrl@prodintec.com

**** Automation and Robotics Section, ESA
e-mail: kjetil.wormnes@esa.int

Abstract

Currently space debris is recognized as a major risk for space missions. In this frame it is involved the Patender project (Net parametric characterization and parabolic flight). The goal of this ESA funded activity (ending by March 2014) is to develop a confident mean to further investigate, develop and validate the concept of using nets for actively removing space debris of different characteristics.

The net simulator will be validated in a parabolic flight experiment where microgravity conditions can be reached during some few tens of seconds. Different net shapes (pyramidal/planar) will be launched using a pneumatic-based dedicated mechanism in order to simulate the capture of a large space debris. High-speed motion cameras will record the experiment in order to allow the 3D reconstruction of the deployment and wrapping around the target phases and the validation of the software simulator.

1   Introduction

In almost 50 years of space activities more than 4800 launches have placed some 5000 satellites into orbit, of which only a minor fraction of about 1000 are still operational today. Besides this large amount of intact space hardware, with a total mass of about 6000 tons, several additional objects are known to orbit the Earth. They are regularly tracked by the US Space Surveillance Network and, today, more than 16 000 of them are maintained in their public catalogue. Only 6% of the catalogued orbit population is operational spacecraft, while 28% can be attributed to decommissioned satellites, spent upper stages, and mission related objects (launch adapters, lens covers, etc.). The remainder of about 66% is originating from more than 200 on-orbit fragmentations which have been recorded since 1961. These are assumed to mainly have generated a population of objects larger than 1 cm on the order of 700 000. The high impact velocities, which can reach 15 km/s for most missions in LEO, are the reason for the destructive energy even despite of the small object sizes. So far, there are four recorded examples of collisions (with the latest and most prominent one between the active Iridium-33 satellite and the decommissioned Cosmos-2251 satellite). Today there is a great concern and consensus that collisions could become the main future source for new debris objects, possibly leading the space debris environment into a chain reaction, rendering some orbital regions with an unacceptably risk for operations. Since the first awareness of the problem in the early 1960s, the global dimension of this problem has been understood today.

Studies at NASA and ESA [1, 2, 3] showed that the environment can be stabilized when on the order of 10 objects are removed from LEO per year with a removal sequence oriented towards the target mass. Active removal can be more efficient in terms of the number of collisions prevented / object removed, when objects removed have high mass, high collision probabilities and high altitudes.

ESA, with its Clean Space initiative, aims at devoting increasing attention to the environmental impact of its activities, including its own operations performed by European industry in the frame of ESA

programs, through the implementation of specific technology roadmaps. The Clean Space initiative organizes the implementation around four distinct branches: 1) Eco-design, 2) Green technologies, 3) Space debris mitigation and 4) Space debris remediation. The main objective of Branch 4 is to start the development and demonstration of the key technologies required for the capture and controlled atmospheric re-entry of an uncooperative target orbiting in the LEO protected region. Currently, a number of technology developments are under-way with many more planned [5].

Over many years, ESA, together with industrial partners, have found throw-nets to be a particularly promising technology for capturing objects in space in cases where robot grasping will be difficult [4, 6] (targets may have unpredictable spins and no suitable grasping points), such as is the case in general for space debris.

The technology development detailed in this paper is funded by ESA's Technology Research Programme (TRP) under branch 4 of the Clean Space initiative, and aims at developing a validated simulator for the capture of large space debris with a throw net, and to demonstrate the capture on a parabolic flight.

This paper is structured as follows: section 1 introduces the space debris scenario and ESA Clean Space initiative, section 2 details the algorithms behind the deployment and wrapping of a space net, section 3 presents the software design of the net simulator, section 4 describes the experimental set-up conceived to validate the net simulator under microgravity conditions with dedicated sections to the parabolic flight characteristics, the scaled scenario, the net launching system, the 3D reconstruction techniques and the proposed validation approach; finally, section 5 summarizes the conclusions of the on-going activity and further steps to be performed.

2   Net modelling

As previously mentioned recent studies have demonstrated that for a future continued use of LEO, five to ten large debris need to be removed every year. For these reasons, the preliminary reference scenario, drawn here, takes as target one of the biggest European LEO satellites, Envisat, to design a tethered-net able to capture and de-orbit Envisat-like spacecraft. The effort is then put in scaling down such a system to an experimental prototype that would be able to faithfully reproduce the former dynamics.

In contrast with rigid capture mechanisms, tethered-net solutions are characterized by capturing debris from a safety distance, by passive angular momentum damping and by establishing a tethered connection between the chaser and the target. Moreover, tethered-nets are general-purpose removal systems: they could effectively intervene on objects different in configuration, materials and possibly in dimensions.

To design a capture net the following design parameters must be taken into account:
- Net configuration, size and mesh.
- Threads diameter and material.
- Bullets masses and launch velocity.

The net configuration deals with the shape of the net, the meshing strategy, the number of bullets, the links to bullets and tether, and strongly depends on the manufacturing technology and the target to be captured.

A net can be conceived either planar or three-dimensional (conical, pyramidal, etc.): for the particular configuration of Envisat the planar net solution has been retained. The number of bullets is here assumed as 4, one per corner no matter the configuration: this bullet number is the minimum necessary to completely deploy the analyzed configuration and it also avoid system fallouts that would appear by increasing the number of bullets. The net size may be related to the debris particular configuration, to increase the wrapping occurrence reliability. In particular, the Envisat case may suggest two different options: either a small planar net, to wrap just the central body of the debris not including the long solar panel in the body envelope wrapped by the net or a bigger net to entirely wrap the object. Bullet masses and initial velocity vectors are considered as optimization variables to get the net completely deployed in the required time and space.

The dynamic modelling of nets has been thoroughly studied for fishing applications [7, 8]: in these studies it is demonstrated how lumped parameters methods are suitable for describing underwater flexible structures as highlighted by the good agreement with experimental results and how such methods allows treating a wide variety of net configurations and initial conditions with low computational costs and stable solutions.

In multi-body dynamics, lumped-parameters methods are widely used, and several studies exist that applies the so-called beads model to space tethers [9, 10]. Generally speaking, a net can be seen as composed by many tethers linked together with knots: in this view, most of the considerations made about tether dynamics modelling are still valid for modelling nets. Furthermore, these methods are intrinsically three-dimensional and can automatically take into account tethers' 3D librations and 3D vibrations. A flexible body can be discretized as series of point masses connected by springs and dashpots. This way the constitutive law of the material can be

modelled through the combination of spring-dampers: the simplest and yet most efficient way to describe the mechanical tension on ropes is the linear Kelvin-Voigt model. It has been obtained considering that an ideal viscoelastic material is represented by the mechanical parallel of a linear spring and a damper. Tension on rope elements can be expressed as (1).

$$T_{ij} = \begin{cases} [-k_{ij}(|\boldsymbol{R}_{ij}| - l_{nom}) - d_{ij}(\boldsymbol{V}_{ij} \cdot \widehat{\boldsymbol{R}}_{ij})]\widehat{\boldsymbol{R}}_{ij} & if \ |\boldsymbol{R}_{ij}| > l_{nom}| \\ 0 & if \ |\boldsymbol{R}_{ij}| \leq l_{nom}| \end{cases} \quad (1)$$

where
- k_{ij} and d_{ij} are the elastic and viscous parameters between element i and j
- l_{nom} is the nominal un-stretched length of the tether element
- R_{ij} and V_{ij} are, respectively, the relative position and velocity between two consecutive masses.

While the damping coefficient needs to be determined experimentally, by using this law the stiffness is directly related to material and rope properties, being the axial stiffness defined as (2).

$$k_{ij} = \frac{EA}{l_{nom}} \quad (2)$$

where E is the Young's modulus and A the thread cross section.

With such a model, the equation of motion for mass i is given by Newton's second law (3).

$$m_i \frac{d^2 \boldsymbol{R}_i}{dt^2} = \boldsymbol{F}_{Gi} + \sum_{j=-1,1} \boldsymbol{T}_{i,i+j} + \boldsymbol{F}_{ext} \quad (3)$$

where
- $T_{i,i+j}$ is the tension between the mass i and i+j
- F_{Gi} is the gravitational force
- F_{ext} is other generic external forces (control, perturbations, etc.).

The contact dynamics have been treated with the penalty method [11]: the contact is resolved a posteriori, i.e. after it has happened. Such a method allows keeping the same explicit ODE structure of the system. It allows a penetration, penalty, between the bodies and responds with a force proportional to such penetration. To avoid penetration of target thin or protruding elements in the net threads, respecting the physics of the phenomenon, a hierarchical bounding-boxes collision detection algorithm [12, 13] has been set-up. It consists of an n-phases algorithm refining the zone of contact, in order to select the specific subsystems of nodes to be cross-checked for collision. This strategy has also the main advantage to speed-up the simulation. In Figure 1 it is possible to appreciate an example of a wrapping sequence.
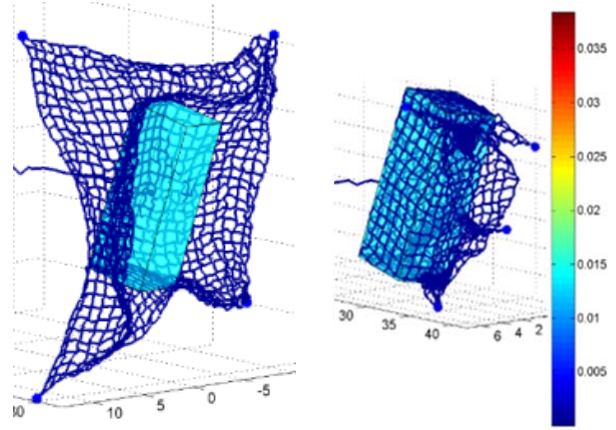

Figure 1 – Wrapping sequence

3 Software simulator design

The net simulator software is decomposed into two main applications: a) Net dynamics and b) Patender GUI application. The net dynamic application is in charge of propagating the net dynamic states along the time, while the Patender GUI application is in charge of providing the user interface for the initial scenario configuration and the 3D visualization during the simulation evolution.

Next Figure 2 shows a layout of the net simulator software architecture.
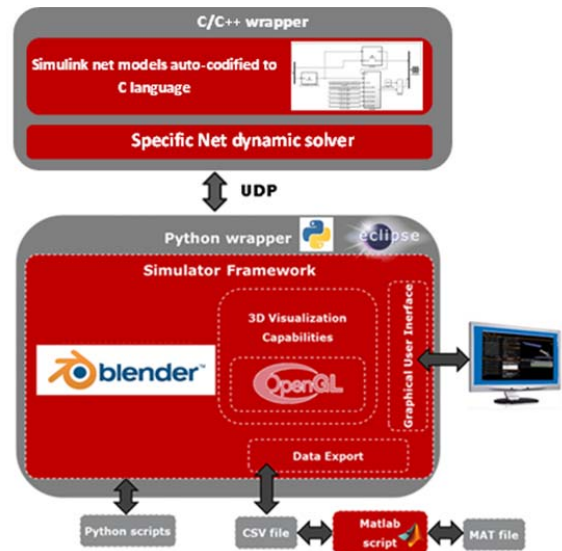

Figure 2 – Net simulator software architecture

Each one of the applications implies an important computational load. For these reason, each application is

separately executed and run on different CPU cores. The communication between these applications is performed via internal UDP packages.

The net dynamic application waits for the configuration and start telecommand coming from the Patender GUI application. In this way, each application is able to be run in different computers. Once the simulation is initialized, the net dynamic application sends the net state (each specific step defined by a decimation factor) to the Patender GUI application in order to display the current scenario. The scenario can then be modified by the user (through Blender interface) in order to create the desired environment for the simulation.

The net dynamic application contains the net mathematical models and the propagator algorithms, which provide the ability of propagating the scenario dynamics from an initial configuration. The net mathematical models are originally implemented in Matlab/Simulink, and autocodified to C-code through the Matlab Embedded coder. The net dynamic algorithms shall be able to propagate large particles systems as well as simple systems. For this reason, after the C-code generation, the algorithms are optimized to manage dynamic memory instead of static memory. The propagator algorithms include a modified solver ode45 implemented in C-code. In order to reduce the excessive computational load of the ode45 solver, it is optimized including the knowledge of the net dynamic behavior.

The Patender GUI application is implemented in the Blender development environment in Python language as depicted by next Figure 3.
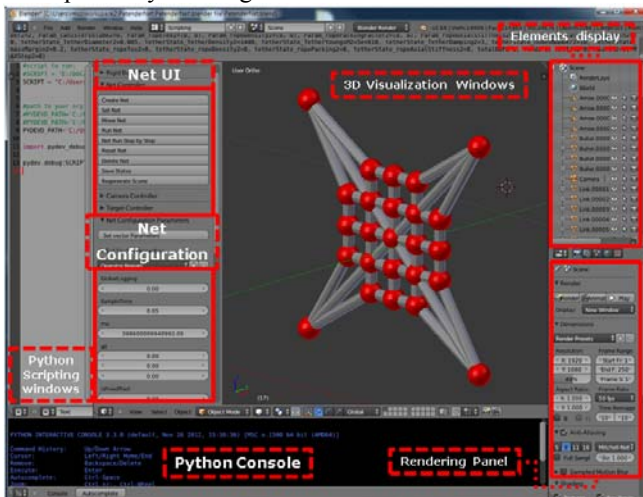

Figure 3 – Patender GUI within Blender environment.

This application includes the graphical user interface (including all menus to load the initial scenario configuration), configuration of the simulator parameters, the 3D visualization capabilities, plotting of the forces and distances between net knot and the capability to export results to CSV format in order to recreate the desired simulation environment. The Python interface is performed to allow the automatic or parametric scripting of simulation from Python commands. It has the advantage of the ability to create new Blender capabilities and group them in groups in order to ease the user use. The use of Blender as simulator framework provides additional facilities to import and visualize several CAD model formats, capability of using for modeling Python scripts. Also provides a broad spectrum of modeling, texturing, lighting, animation and video functionality, and exploits the Blender/OpenGL rendering engine motor.

4 Experiment set-up

4.1 Experiment description

The foreseen deployment of the net and wrapping of a satellite mock-up will be performed within an experiment cabin of 3x1.5x1.5m installed on the cargo area of the parabolic flight aircraft provider. Several nets (two-three) will be deployed at two different velocities during at least 18 Zero-G parabolas with a typical duration of 20s. The experiment will be autonomously recorded by four high-speed video-cameras to allow further validation of the software simulator against the recorded motion of the nets.

4.2 Scaled scenario

The scalability is a powerful tool to experimentally investigate phenomena the modelling of which need either refinement or validation. In fact, the scalability entails the similitude exists between a model and a prototype, being the model the physical element tested in laboratory and the prototype the element in its actual size and operational conditions.

In particular, a complete similitude means the dynamics occurring on the model is a scale of the dynamics occurring on the prototype, enabling analyzing a phenomenon in laboratory and correctly reporting it to the actual size application.

The size of the net has been scaled according to the Buckingham π theorem and by taking into account the parabolic flight envelope and the foreseen deviation of the floating object (net) relative to the fixed object (target) during parabola.

The net design for the parabolic flight foresees two nets of different dimensions (0.9 x 0.9 m and 0.6 x 0.6

m) weaved in Technora black twines. Such dimensions allow with a single target mock-up to test two different strategies of capture: one that wrap the whole mock-up (body plus solar panel) and one that only wrap the bus body. Therefore the two net are representing two different prototypes, basically working different in the capturing phase.

A quadrangular mesh has been selected for the net, as visible in Figure 4: this topology revealed to be the best compromise between total mass and out of plane stiffness. Square mesh has also the ability to withstand large shearing deformations without requiring creases in the material, which is an important characteristic for folding and packaging. The nets are given reinforced threads in the diagonals, perimeter and medians, that are never interrupted and become load paths. Reinforcements are necessary for the net prototype to withstand loads during orbital maneuvers without unacceptably increasing the mass of the whole net: the reinforcements influence the dynamics behavior of the net and have been retained in the scaled model to be consistent with the representation of the prototype dynamics. The main driver that led the selection of threads diameters for the experimental purposes is the possibility to be seen by optical sensors (cameras). The minimum static spatial resolution is in fact slightly above 1 millimeter, resulting in diameters under the millimeter non acceptable. The same ratio between yellow and green threads diameter (Figure 4) coming from the prototype sizing, has been retained.
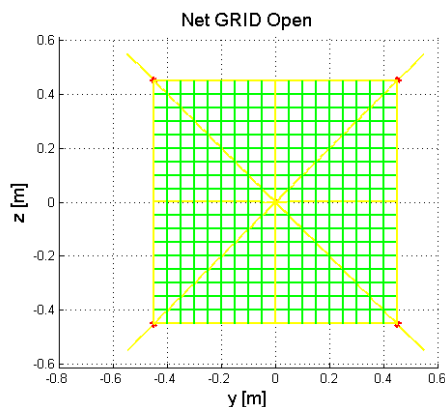

Figure 4 – Quadrangular mesh net with reinforcements

An effort has been put in scaling the net by keeping the same diameter scale and varying only the macro lengths such as size and mesh: in this way the linear density can be decoupled from the threads cross area and the scaling procedures relies on the other free parameters.

The folding of the net inside the canister is at the same time a key point and major issue. A deployment is strongly dependent on the initial folding of the net, meaning that a successful deployment requires an adequate folding pattern; the folding in fact corresponds to the initial conditions of the net and the correspondence between simulation and experiment shall be as close as possible to get fine results. The boundary conditions depend, in some sense, on the folding since some parts of the net constrain others from moving. However, net folding, especially if done manually, will always be affected by a high degree of uncertainty, also due to the fact that the net is not folded and kept in vacuum but it may move during the ascent/descent between parabolas. The drivers for an effective folding pattern choice are to place the vertex at the bottom of the canister and the mouth at its top near the cover to allow correct initial conditions for deployment. Another important driver is to keep the symmetry as much as possible.

4.3 Net launching system

During the experiment under micro-gravity conditions, the net launching system will enable to carry out net launching operations. This net launching system is composed of several parts: a support and a motherboard where the rest of elements are integrated (see Figure 5).

Figure 5 – Complete net launching system (left) and canister container closer view (right)

The structure of net launching system is based on a metallic table composed of two parts. The first one is a support table resting on the ground by four supporting points. The second one is a turning plate whose purpose is enabling angular placement of the motherboard to ease the direction of the net launching throughout experiment. This turning plate includes two hinges, a key and a cog and it allows 180º rotations (by increments of 15º). Over such turning plate it is placed a motherboard where the rest of the elements are integrated. These elements are: four bullets, four bullets liners, four angle-adjusting mechanisms and a net container support. Besides, it includes a structure made of aluminum profiles (metallic joint) in order to fix the storage tank, the support table and an electrical connections box.

The mechanism to adjust the launching angle of the bullets can be operated independently for each bullet. It allows an angle range from 15º to 45º, measured from the vertical line / axis. Bullet liners are the mechanical guidelines where bullets are placed. Through these liners, the pressurized air flows out inducing the ejection of the bullets and consequently of the attached net. These bullet liners include bearing bushes made of non-slip material to guarantee that friction stresses are negligible.

Bullets have been designed considering the type of net. Key features are geometry, mass and center of gravity. These design criteria allow bullets to be pushed away over the bullet liner by means of pressurized air. The contact point between the air flow and the bullet must be located under its center of gravity in order to ensure a longitudinal motion. The pressurized air flow is activated by electrical/pneumatic system.
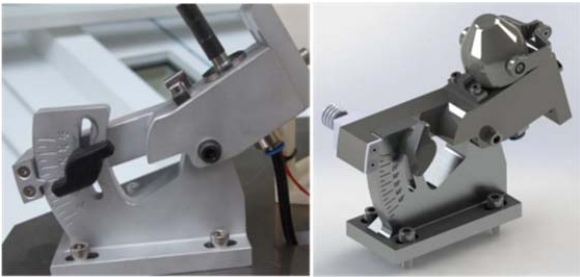

Figure 6 – Angle adjustment system, bullet liner and bullets

Canister or net packing container is the element where the packet net will be placed. Additionally, this canister will be placed inside its support by an adjustment system. The canister is placed in the support and its position is fixed thanks to lateral jugs and magnets. This approach allows placing several types of containers depending on geometry requirements of the net.

The net launching system includes a cover over the canister and its corresponding opening system. The cover is integrated in the container support and it is articulated without interfering with the ejection of the bullets. This articulation is made of a set of antifriction bearing bushes to permit an easier turning. The cover is opened due to the force of two torsion magnets (torsion springs). This force is constant until the locking system of the cover is opened. The cover opening is triggered by a dedicated delayed relay of the electrical system.

Next Figure 7 shows the pneumatic scheme of the net launching system.
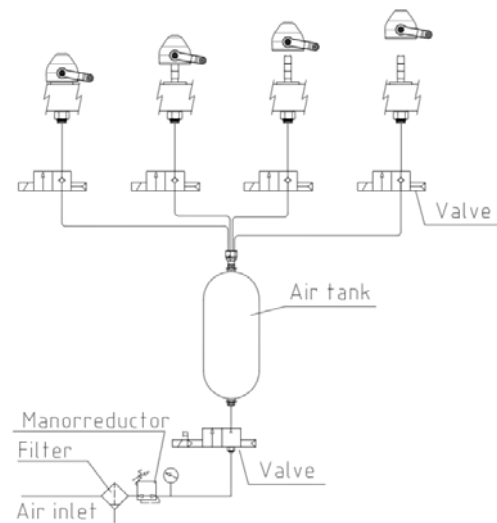

Figure 7 – Pneumatic scheme

The pneumatic system is controlled by an electrical system composed by several relays and activated externally by a remote control in the hands of the operator. The feeding air flow is under air pressure and it goes through a filter to be ready to go to the manometer. After going through the manometer, the pressured air flow is under desired pressure within selected pressure range. Then, the air flow is directed to the V5 valve to fill the air tank. Afterwards, when the bullets launching is carried out, the pressurized air flow is divided into four lines to reach the four bullets valves (V1, V2, V3 and V4). After activation of such valves the bullets are pulled by means of the pressurized air through bullets liners.

Due to the timing constraints imposed by the parabolic flight characteristics, the net container has been designed as an independent element from net launching system. As result, a reload or charge/discharge tool has been designed to ease operator tasks and optimize the time between parabolas. This reload tool (see Figure 8) allows an easy assembly of bullets and net into the canister.

Figure 8 – Operating handling the net reload tool

4.4 3D net trajectory reconstruction

The following aspects needed to be carefully investigated in designing the imaging acquisition line for the experiment: a) image quality versus frame rate, b) recording time and memory, c) cameras location and field of views and d) illumination conditions.

The illumination conditions deserves an important remark since the measurement set up takes advantage of high-speed instruments. Being the shutter really quick it is fundamental to provide the measurement environment with intense light source inside the experiment box. These light sources are located along the test box longitudinal edges (not facing any camera) in order to provide uniform light condition and avoiding shading of objects. It is also important to ensure the adequate contrast of the objects onto the background. In fact the features detection phase during the post process of images is crucial to obtain a good reconstruction result. A uniform white background has been arranged to maximize light reflection and to make the object of interest stand out: the interest points on the net are color-coded to set up visible markers on the net knots. To process images, in fact, it is fundamental to precisely locate markers and detect their pixels coordinate at each frame. A trigger device is provided to trigger all the cameras at the same time within the experiment. The precise synchronization is performed a posteriori through the use of a flash light pulse at the activation of experiment to set epoch 0.

The minimum number of viewpoints to reconstruct a three-dimensional motion in a three-dimensional environment is two: in fact the combination of two images of the same point taken from different positions, whose relative location is known, makes possible to solve the triangulation problem and to locate the point in space, with respect to a fixed object in the scene. Here, the experimental set-up takes advantage of 4 SONY NEX-FS700 recording FULL-HD videos up to 240 fps. The choice has been to exploit the advantage of having a double stereo location of the cameras in order to combine the benefits of having stereo systems (mostly for post-processing reasons) with the multi-view option, allowing to have two quasi-orthogonal axis of view (to further reduce the reconstruction error). A preliminary sketch of camera locations (cyan triangles) in the experimental box is visible in

Figure 9, along with the nominal deviation of the free-floating object (i.e. the net in yellow) during the parabola, with respect to target mock-up (in red).
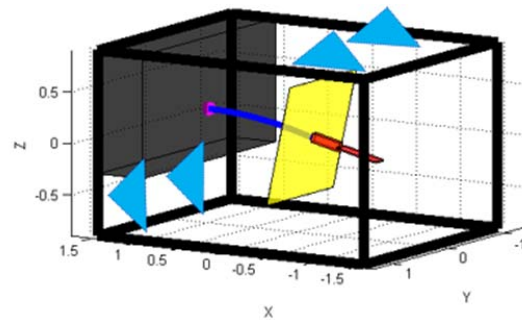

Figure 9 – Experimental box diagram

The most important advantage of using input of video sequences is the higher quality one can obtain. Both geometric accuracy and visual quality can be improved by exploiting the redundancy of data. Image sequences also enable some techniques to deal with shadow, shading, and highlights [14, 15]. However, to fully take advantage of the use of video sequences one have to deal with some problems, ranging from pre-processing (frame selection, sequence segmentation) to post-processing (bundle adjustment, structure fusion). Among a number of frames, selecting good frames will improve the reconstruction result.

4.5 Simulator validation

The net simulator validation is understood as the main goal for the present activity. This validation will be performed after the parabolic flight experiments campaign, and the process will be based on comparing the experimental data with the expected data (obtained from the Net Simulator output). The key magnitude to be compared during the validation process is the net particles position (knots and bullets), and the error will be estimated from standard deviation along the time.

A sensitive analysis of the Net Simulator is required in order to define appropriately the key parameters of the validation process and the parabolic flight experimental campaign (net configurations, number of experiments for each net configuration, parameters to be modified between experiments…).

The nominal range sensitive is the most common method due to the simplicity in the implementation and the effectiveness. However, the Net Simulator includes several parameters to be analyzed. For this reason, the automatic differentiation technique will be considered. This method is an automated procedure for calculating local sensitivities for large models. In automatic differentiation technique a computer code automatically evaluates first-order partial derivatives of outputs with respect to small changes in the inputs.

5   Conclusions

The use of throw-net to capture space debris seems to be promising being a general purpose mechanism partially independent from target motion and physical characteristic. The implementation of a validated simulator is needed to design a reliable operational device. The output of this activity will be the implementation of such a simulator and its validation through a parabolic flight campaign when the motion of a scaled net wrapping a target mock-up will be recorded in super-slow motion mode by four synchronized high-speed video cameras. The 3D trajectory of relevant points will be then reconstructed using stereo matching and triangulation and later compared to simulated values to perform model validation and update.

Preliminary on-ground tests have already proved the capability of the described pneumatic system to deploy a polyethylene net and the feasibility of reconstructing bullets motion by means of high-speed video-cameras (see Figure 10).
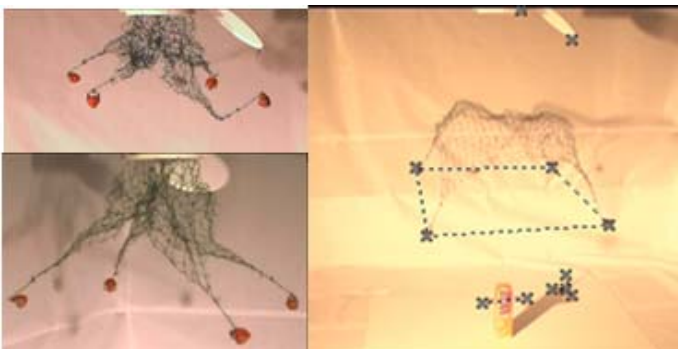

Figure 10 – On-ground vertical downwards net deployment

Further work is devoted to on-ground testing of lighter nets made of Technora fiber and their corresponding 3D motion reconstruction. Such results would allow performing a preliminary validation of the software simulator before testing the experiment in microgravity conditions during a parabolic flight.

References

[1] J.-C Liou and N.L.Johnson, "Risks in space from orbiting debris", Science, 311(5759): 340–341, January 2006.

[2] B. Bastida and H. Krag,"Analyzing the criteria for a stable environment", AAS/AIAA Astrodynamics Specialist Conference, Girdwood, Alaska, July–August 2011.

[3] J.C. Liou and N.L. Johnson, "A sensitivity study of the effectiveness of active debris removal in LEO", IAC-07-A6.3.05, Hyderabad, India.

[4] "Robotic Geostationary Orbit Restorer", GSP phaseA final report, Astrium SI, Bremen, June 2003. Doc no: ROG-SIBRE-FP.

[5] K.Wormnes, et.al., "ESA technologies for space debris remediation", 6th European Conference on Space Debris, Darmstadt, 2013.

[6] K.Wormnes et.al. Throw-nets and tethers for robust space debris capture, In IAC2013, Beijing, October 2013.

[7] C. Lee, B. Cha, and H. Kim, "Physical modeling for underwater flexible systems dynamic simulation", Ocean Engineering, pages 331-347, October 2005.

[8] K. Suzuki, T. Takagi, T. Shimizu, T. Hiraishi, K. Yamamoto and K. Nashimoto, "Validity and visualization of a numerical model used to determine dynamic configurations of fishing nets", Fisheries Science 2003; 69: 695–705, January 2003.

[9] P. Williams, "Dynamic multibody modeling for tethered space elevators", Acta Astronautica 65 (399-422), 2009.

[10] V. S. Aslanov, A. S. Ledkov, "Dynamics of tethered satellite systems", Oxford, Woodhead, 2012.

[11] G. Hippmann, "An algorithm for compliant contact between complexly shaped surfaces in multi-body dynamics", Institute of Aeroelasticity DLR – German Aerospace Center, Wessling, Germany.

[12] G. Zachmann, "Virtual reality in assembly simulation – Collision detection, simulation algorithms and interaction techniques", PhD thesis, Department of Computer Science, Darmstadt University of Technology, 2000.

[13] M. Woulfe and M. Manzke, "A Framework for Benchmarking Interactive Collision Detection", Trinity College Dublin, Budmerice, Slovakia, April 2009.

[14] "Visual 3D Modeling from Images", Pollefeys M. Notes, University of North Carolina, Chapel Hill, USA.

[15] "Visual modeling with a hand-held camera", Pollefeys M. International Journal of Computer Vision, 59:207–232.